

EXPERIMENTAL MEASUREMENTS OF VELOCITY THROUGH GRANULAR-LIQUID FLOWS

N. SANVITALE^(*), E.T. BOWMAN^(**) & R. GENEVOIS^(***)

^(*)University of Padua - IMAGE Dept. - via Ognissanti 39 - 35129 Padova, Italy - e-mail: nicoletta.sanvitale@unipd.it

^(**)University of Canterbury - Department of Civil and Natural Resources Engineering, Christchurch, New Zealand

^(***)University of Padua - Department of Geosciences, Italy

ABSTRACT

This paper describes a series of “small scale” laboratory flume tests designed to examine the motion and arrest of concentrated granular-fluid flows, with a view to understanding debris flows. A non intrusive optical approach which relies on the matching of the refractive index and the planar laser-induced fluorescence techniques (PLIF), is adopted to analyse the flow behaviour of a granular medium in a ‘free surface’ condition and in the context of relatively high-speed movement. A PIV (Particle Image Velocimetry) approach, adapted for geotechnical testing, is used to measure the velocity profiles as obtained from laser-illuminated images through the transparent flowing granular material. PIV analyses of experiments carried out using two different mixtures, one characterized by well-graded and one by uniform particle size distribution, are compared in order to understand the effect of the granular composition on the flow dynamics. The experimental results suggest that the particle size distribution has an influence on the mobility of flowing granular material at a given moisture content. Flow of well-graded mixtures show higher velocity, smaller flow thickness and a larger run-out extent. The velocity profiles of the two mixtures, measured at the control section of the flume slope, exhibit different behaviour with a lower degree of shear for that with uniform particle size distribution.

KEY WORD: debris flows, physical modelling, flume study, PLIF, granular-fluid flows, PIV analyses

INTRODUCTION

The mechanics of concentrated granular-fluid flows is characterized by momentum and energy transfer caused by inertial grain collisions, grain contact friction, viscous shear and solid-fluid interactions (IVERSON, 1997). Constitutive equations for such flows are not completely defined and detailed experimental observations represent a key tool to understanding their kinematic behaviour. Physical modelling of granular-fluid flows moving down an inclined flume provides an important approach to understanding geophysical granular flows like debris flows and mud flows.

Usually in debris flow experiments it is possible only to examine the behaviour at the flow margins (the top and the sides) since the ability to probe the internal behaviour of concentrated two-phase flows is prevented by their high opacity. Experimental evidence shows that the dynamics of the inner part of the flow can be different from the motion close to the sidewall (ARMANINI *et alii*, 2005). That is, the two dimensional nature of the sidewall measurements can only partially represent the three dimensional features of the flow inside the bulk. Past experimental studies analyzed the internal characteristics of grain-fluid mixtures. MAINALI & RAJARATNAM (1994) measured velocity and concentration profiles for a highly concentrated sand-water slurry, sampling the flow in the centre of the flume. Velocity profiles of the entire flow field of mudflows in a recirculatory flume were

obtained using a pulsed Doppler ultrasound technique by ARMANINI *et alii* (2003).

A well-known technique to achieve optical accessibility to the inner parts of particle-liquid medium can be obtained by matching the refractive index of transparent solids and fluid. Optical matching makes the entire mixture transparent allowing investigation of the internal points. Combining refractive index matching with planar laser-induced fluorescence (PLIF) techniques enables the visualization of deformation within a saturated granular flow and enables the use of deformation measurement techniques, such as Particle Image Velocimetry (WHITE *et alii*, 2003).

A number of studies have used the matching of refractive indices to achieve optical accessibility to liquid flow phenomena (BUDWIG, 1994), and their application to porous media using PLIF has been undertaken by MONTEMAGNO & GRAY (1995); FONTENOT & VIGIL (2002), STOHR *et alii* (2003); ORPE & KUDROLLI (2007).

In this paper we present the preliminary results obtained by applying the aforementioned techniques to the analysis of fast moving granular-liquid flows in a small scale flume. In the model described here, data are extracted from 2-D vertical sections through the flowing granular material. The physical and optical properties of the selected solid and liquid, and the adopted methodology are presented. Further, the results of the first experiments are discussed with particular attention to the measurement of the velocity profiles.

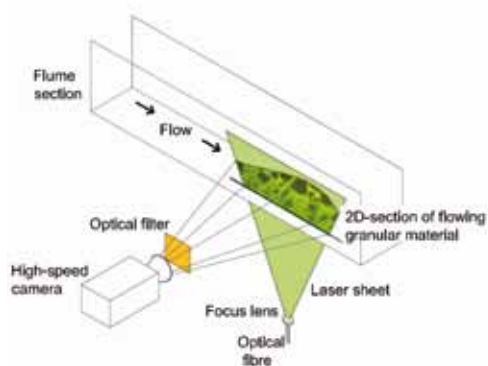


Fig. 1 - Schematic layout of the adopted PLIF configuration

METHODOLOGY

Matching the refractive indices of the components of a solid-liquid system should render the mixture transparent and the investigation of its inner parts possible. In order to distinguish the solid particles in the fluid, a fluorescent dye is added to the fluid phase. The dye is excited by a laser light with a wavelength tuned to its absorption band. As soon as the dye de-excites (on the order of nano to microseconds), it emits light at a wavelength larger than that of excitation. This light, known as fluorescence, enables the observations of both geometry and deformation through the particle-fluid system: the particles in an image appear dark against a bright background, as shown in Fig. 1.

EXPERIMENTAL APPARATUS

The experimental set up is shown in Fig. 2. The main experimental device is a small scale flume with an aluminium head tank containing the flow material above the top of the slope. A curved chute guides the flow from the mouth of the tank to the top of the slope, at which point the flow travels down a 150mm wide by 2000mm long channel before being deposited on a horizontal runout surface. The slope angle can be varied from 0° to 40°. The bottom of the channel is made of stainless steel which is artificially roughened over the last 1m by means of a synthetic material with a slip resistant surface (3M Safety-Walk 370). The outward facing walls are made from Perspex except for the part corresponding to the rough bed, which is made of borosilicate glass. A high-speed digital camera (SVSi Memview) records the downslope flow behaviour through the glass sidewalls. Before its release, the prepared saturated material is stored in the head tank and continually agitated to ensure that the least possible segregation and consolidation takes place before the release of the material. The pneumatically-operated tank trapdoor is linked by a micro switch to the high speed camera to ensure a time-delay between the release of the material and recording of the flow. The frame rate of the camera is set at 1100 fps.

LASER LIGHT SOURCE AND OPTICAL DEVICES

The light source is a 800 mW solid state laser (Changchun New Industries) at a wavelength of 532 nm. The laser beam is coupled into an optical fibre, recollimated at the fibre output, and then sent through

a Powell lens generating a vertical sheet of light with a thickness of around 2 mm. In some preliminary experiments, the laser sheet illuminated the flowing mixture from above, but the interaction between the incident light and the surface of particles protruding from the free surface of the flow was found to cause distortion of the planar laser beam. This resulted in a broadening of the laser sheet and in the illumination of particles outside of the intended measurement plane focused on by the camera (SANVITALE *et alii*, 2010).

Modifications of the experimental apparatus were made to apply the laser sheet from beneath the flow through the bottom of the channel. The steel base in the distal part of the channel (1 meter before the exit point to the runout area) was replaced with a standard glass plate. Then the upper glass surface was covered by means of the same synthetic material to provide the necessary roughness. A slit, 300 mm in length and 1.5-2 mm wide, cut through the rough material was made to let the light pass through the base. With this altered set-up the high-speed camera can record the images of each flow along a laser illuminated longitudinal plane passing through the slit. The illuminated plane is located 35 mm from the sidewall and begins approximately 110 mm before the exit point of the flume channel to the horizontal deposition area. The final set-up is shown in Fig. 2.

SOLID, FLUID AND DYE PROPERTIES

There are several key concerns in choosing appropriate pairings of transparent particles and associated fluids. They must be optically compatible in terms of refractive index, reasonably economic and non-hazardous to work with. Borosilicate glass (Schott Duran®) is used as transparent material for the solid particles. A hydrocarbon oil (Cargille Immersion Liquid code 5095) is used as fluid phase.

This liquid closely matches the index of refraction of Duran at the dye emission wavelength and at a temperature of 22-24°C. The optical and physical properties of these two materials are reported in Table 1. The borosilicate glass has been purchased from the manufacturer in rods with diameters from 4mm to 30 mm and tubes with wall thickness ranging from 0.8 mm to 2.0 mm. The tubes are crushed to obtain particles smaller than 4.5 mm whereas the coarsest particles up to 30 mm are cut from the rods in cylindrical pieces and subsequently shaped in order to achieve an irregu-

lar shape. The particles with size larger than 30mm have been made by smashing a 28x15x6 cm block of Pyrex® glass (Dow-Corning), a borosilicate glass with the same optical characteristic of Duran but of a different brand (no longer produced).

In order to create a distinction between fluid and solid, the fluorescent dye Nile Red (Sigma-Aldrich) is used. This dye is soluble in non-aqueous phase and shows a meaningful quantum efficiency and absorption rate at the laser excitation wavelength. These properties are necessary to achieve a high intensity of emitted light, which is fundamental to capturing im-

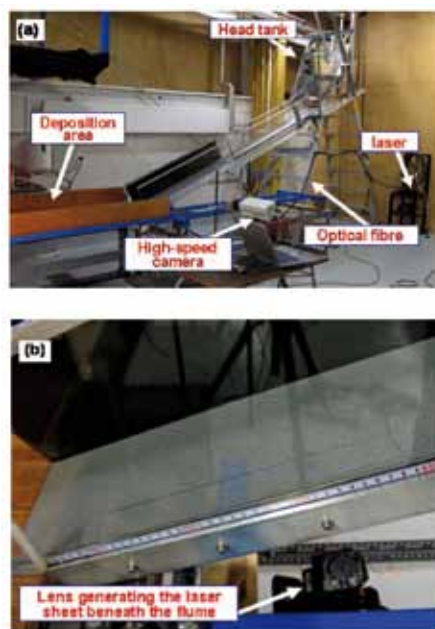


Fig. 2 - Experimental set up with laser

	Refractive index at 589.3 nm	Density at 25 °C (g/cm ³)	Kinematic viscosity at 25 °C (m ² /s)
Hydrocarbon oil (Cargille 5095)	1.4715 (at 25 °C)	0.846	16e-6
Duran® glass	1.4718 (at 21 °C)	2.23	-
Soil	-	2.65	-
Water in debris flow	1.3333 (at 20 °C)	1.00	1-10e-6 (dependent on clay content)

Table 1 - Solid and fluid properties

Particle Size Distribution	C_U	C_z	D_{90} (mm)	D_{50} (mm)	D_{10} (mm)	Number of tests
PSD9-mod	20.2	1.1	35.5	7.1	0.54	2
PSD16-up	3.3	0.9	17.6	7.1	2.7	2

D_{10} and D_{50} , effective and mean grain size; D_{90} , particle size for which 90% of the particles are finer; C_z , coefficient of curvature; C_U , coefficient of uniformity.

Table 2 - Properties of employed particle size distributions

ages at a high frame rate during the experiment. During the tests a longpass filter (Schott OG550), with the cut-point at 550 nm, is placed over the camera lens to transmit the fluorescence signal and screen unwanted scattered light.

TEST CONDITIONS

Debris flows are mixtures of granular sediment and fluid, with both components influencing the resulting flow and deposition behaviour. Field evidence shows that virtually all debris flows contain a wide particle size distribution (PSD), with sizes ranging from boulders or gravel to silt and clay. The typical mean particle size D_{50} ranges between 2 mm and 200 mm while the values of the uniformity coefficient $C_U = D_{60}/D_{10}$ are of the order of 100-1000 (e.g. HURLIMANN *et alii*, 2003; PIERSON, 1980).

Usually, experimental flows are characterized by a mean particle size which is necessarily smaller than that found in the field, and use a relatively uniform PSD ($C_U < 5$). Important aspects of their behaviour, such as segregation of the particles and high mobility, are unable to be replicated in such tests. Experimental research (BOWMAN & SANVITALE, 2009) has shown that the particle size distribution has a significant effect on the mobility of flowing granular materials at a given moisture content, and small laboratory flume tests can reproduce key aspects of the debris flow behaviour if a careful selection of the material, in terms of gradation and particle size, is made. In order to analyze the influence of a change in the value of C_U (at a given mean particle size D_{50}) on the kinematic behaviour of granular-liquid mixture, for the results reported herein, two particle size distributions, namely PSD9-mod and PSD16-up, were chosen (Fig. 3). Table 2 summarizes the main parameters of the adopted solid material.

For both the PSDs two experiments were carried out to ensure repeatability of results. In each run, a mixture prepared with 12 kg of glass particles satu-

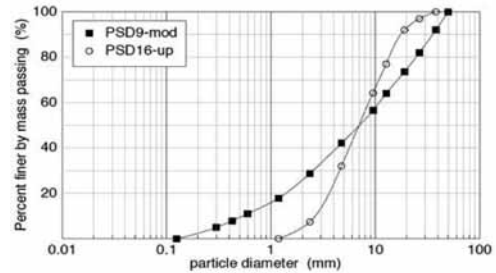


Fig. 3 - Particle size distributions used for the experiments

rated with 3.94 litres of oil was used, for a resulting overall sediment volume concentration of 0.57. The concentration of the Nile Red in the oil was 2.5 mg/l, the laser power was set around 600 mW and the frame rate of the camera at 1100 fps. The flume slope angle was 24.5°.

VELOCITY MEASUREMENTS

Measurements of the velocity profile inside the flow were obtained using GeoPIV software (WHITE *et alii*, 2003). GeoPIV operates by tracking the texture (i.e. the spatial variation of brightness) of sub-regions in an image, often called “patches”, in multiple images. The displacement vector of each patch in the time interval occurring between two subsequent images is found by locating the peak of the autocorrelation function of each patch.

The original GeoPIV algorithm has been modified by W.A. Take (private communication) to the needs of the present work, by supporting a static mesh, with position and geometry fixed in the image and through which particles flow. Each mesh consists of a single column of patches. The patches overlap in the vertical direction at a spacing of half of the patch size. The displacements are calculated at two subsequent time steps (i.e., two subsequent frames), providing an estimate of the instantaneous velocity field at the mesh location.

For these experiments, velocity fields were estimated at regular time intervals (60-90 frames, corresponding to 0.054-0.082 s), by defining a static mesh covering the entire height of the flow, as shown in Fig. 4. For all the tests, the first mesh was placed immediately after the unsaturated coarse front, where fully saturated conditions made the PLIF technique effec-

tive. Square patches with two different sizes, 16 or 32 pixels (1/16 or 1/8 of the image height), were used. The former allowed a higher spatial resolution to be obtained, and hence more detailed, although more noisy, results. The latter led to more precise results but at the expense of resolution. For each patch, the velocity was calculated as the mean of the instantaneous velocities estimated over 30 successive frames (corresponding to a time step of 0.027 s). Figure 5 shows an example of the distribution of the velocity estimates obtained at each patch both for the x (horizontal) and the y (vertical) components. This velocity is an in-plane velocity, and the x and y axes are oriented in directions parallel and perpendicular to the mean flow direction, respectively. The vertical velocity was found to be at least one order of magnitude smaller than the horizontal one and therefore, its contribution was neglected in the analysis presented here. The standard deviation was calculated for velocity at each depth and values falling outside a proper confidence interval were neglected and the mean recalculated accordingly. For patches of 32 pixels (hereafter called 32pix), the confidence interval was set to three standard deviations, while for patches of 16 pixels the confidence interval was set equal to one standard deviation, in order to cope with the large scattering associated with the corresponding data.

RESULTS

DEPOSIT MORPHOLOGY

Figure 7 shows photos of the deposit fan for both PSD. Both of the experiments carried out for each PSD exhibited approximately the same shape and runout, with differences in length smaller than 10%. The largest runout lengths were found for the experiments with the highest values of C_U , i.e. for

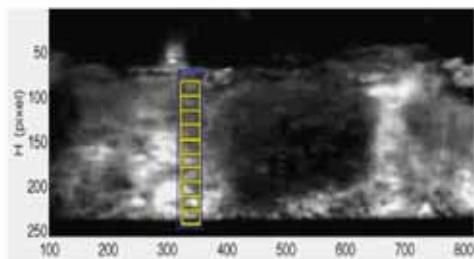


Fig. 4 - Example of static GeoPIV mesh

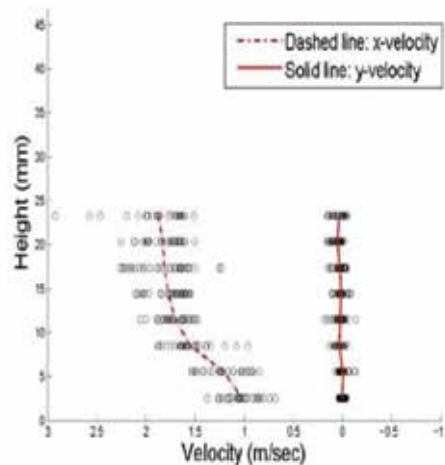


Fig. 5 - Example of measured velocity profiles for the body of the flow. Each dot represents the velocity estimate resulting from the comparison of two subsequent frames. The continuous lines are the velocities calculated as the mean of these instantaneous velocities

well-graded materials. These tests also displayed the greatest overall segregation during flow and deposition. The deposits on the runout area exhibited morphologic features common to many natural and laboratory debris flow fans (MAJOR & IVERSON, 1999) with coarse particles concentrated at the front and at the outermost margins, while the finer material was emplaced at the rear of the fan. Figure 6 shows an example of the resulting particle size distribution of three samples collected at the front (“lobate” part of sample) and in the middle (“centre” of sample) of the runout zone for each PSD. We also collected a sample at the distal part of the flume (“flume” sample), where some material deposited before reaching the horizontal runout area. Both the replicates carried out for each PSD showed essentially the same morphologic characteristics in the deposit zone.

IMAGE ANALYSIS

Digital images of the flows are shown in Fig. 8 and Fig. 9. The flow proceeds from left to right and the camera is angled so that the base of the channel is parallel to the base of the camera in the images. Figure 8 shows images resulting from an experiment with the well graded particle distribution (PSD9-mod). The flows obtained using these gradations were thin and elongated. A few bouncing grains preceded the arrival of the front. The snout, consisting of coarse parti-

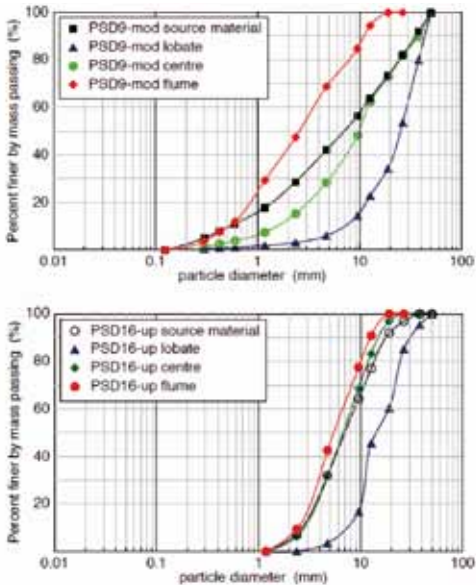


Fig.6 - Examples of the particle size distributions for the lobate, centre and flume sample for each PSD

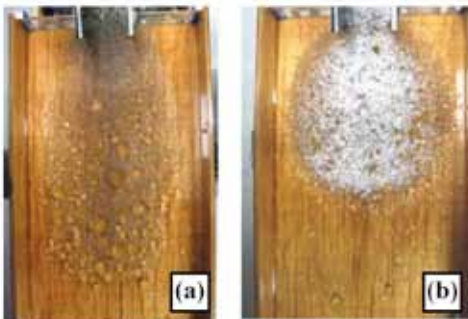


Fig. - Photos of runoff zone after the test (a) PSD9-mod; (b) PSD16-up

cles, had a velocity at the control section larger than 2 m/s. Both the front and the following body of the flow had approximately the same height, around 25-30 mm. The depth at the tail of the surge was around 10 mm. The flow segregated during motion with most of the coarse particles concentrated towards the front. Through the depth, the segregation was not so evident, due the small thickness of the flow in comparison to the average size of the grains. Nevertheless, the tendency of the coarse particles to position close to the free surface is visible in Fig. 8, many of them (mostly the largest) appearing to “float” on it.

Figure 9 shows the images from a test using

PSD16-up. The flow behaviour was different from that of the well-graded mixtures. The entire flow was short and moved as a bulk. The front had a thickness of around 70 mm, greater than the height of the camera image, while the thickness of the tail was around 10-20 mm. From the images, the degree of segregation appears to be lower, with coarse particles present also in the body of the surge. The front was unsaturated (individual particles are visible as illuminated block and not as dark spot since PLIF needs fully saturated condition to be effective) and highly concentrated. Due to a significant number of air bubbles it was not possible to obtain clear images of the front. The penetration of the laser within the flow close to the front was partially prevented by the high concentration of the particles and the large thickness of the medium (with the output laser power decreasing with the distance). The resulting images are blurred and not clear. The level of detail improves significantly towards the tail, where the solids concentration progressively decreased. The average velocity of the snout was approximately 1.5 m/s.

MEAN VELOCITIES

Two experiments, one for each PSD, have been analyzed. The analysis starts from the part of the flow where fully saturated conditions make the PLF technique effective, emphasizing the solid particles as black spots against a bright background. Figure 10 shows the time evolution of the mean flow velocity. This is calculated for each mesh, placed at different positions in the flow, as the average of the mean velocity estimates of its patches. In Fig. 11 the estimated heights of the two flows obtained by plotting the position of the highest patch of each 16 pix mesh are shown. Note that this is just an approximation of the true height, since the meshes cannot cover the entire depth of the flow. This is due to the restrictions posed by the software, which requires that the top patch of the mesh must be set just below the free surface. It is useful for the following discussion, to distinguish between two main regions for each flow, defined as the “body” and the “tail”.

For PSD16-up, the body is defined as the region showing the highest thickness and the largest mean velocity: it occurs within the interval between 0 and 0.36 s (see Fig. 11). The remaining part of the flow, with decreasing height and velocity, represents the

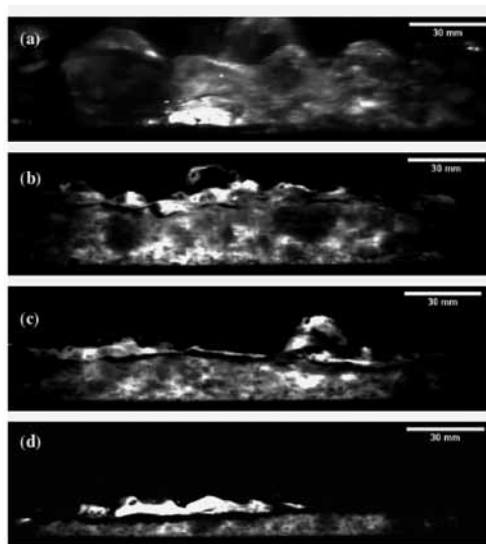


Fig. 8 - Digital images of the test using PSD9-mod. The flow is proceeding from left to right. (a) During arrival of the flow front; (b) In the body immediately after the front; (c) In the core of the flow; (d) In the tail

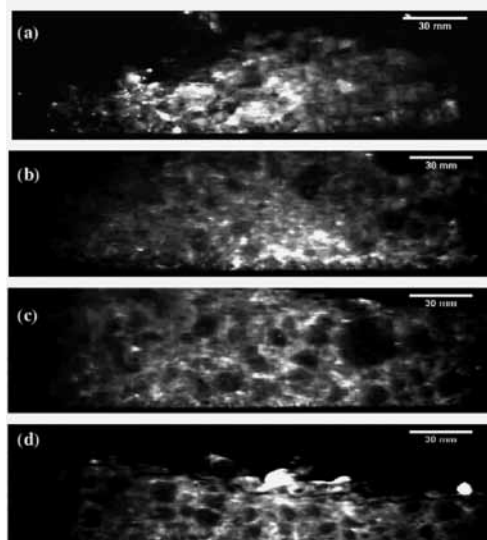


Fig. 9 - Digital images of the test using PSD16-up. The flow is proceeding from left to right. (a) During arrival of the flow front; (b) In the body immediately after the front; (c) In the core of the flow; (d) In the tail

tail. For PSD9-mod, the body is identified between 0 and 0.45 s. This part of the flow exhibits a high (except for the first two mesh positions) and rather constant thickness (see Fig. 11). In the body the velocity is high and, although fluctuating, slowly decreasing (see Fig. 12). The tail is initially characterized by a fast decrease of the velocity and height, which progressively becomes gentler.

Comparing the experiments, the most uniform material (PSD16) moves with a lower velocity at any time, even if at the end of the flow (in the tail) the velocity of both the tests is comparable. A particular feature of the PSD9-mod velocity curve is represented by large ripples at the initial part of the body. Such ripples are not the result of numerical noise, but they seem

to be related to the presence of large particles, whose size is comparable with the flow thickness as shown in Fig. 4. These particles, which move faster than the surrounding matrix, preferentially at the surface of the flow, occupy a significant part of the available space and seem to push and accelerate the material immediately in front of them. Further analyses of other tests with similar features (i.e. a well-graded mixture with some large particles inside the flow) need to be performed in order to elucidate this behaviour.

The height profiles confirm that PSD16-up moves as a bulky surge, with a thickness significantly larger than that of PSD9-mod. The heights of the flow drop suddenly at the beginning of the tail, decreasing from about 55 mm to less than 10 mm. The well graded mixture (PSD9) has a reduced thickness which decreases smoothly toward the tail. Some examples of the estimated velocity profiles are presented in Fig. 12. For both PSDs, two profiles from the body (a and b) and two from the tail (c and d) are shown. The mean values and the corresponding errors bars (standard deviation) are plotted for 16 pix meshes (blue lines). The velocity obtained from 32 pix mesh is overlapped for comparison. The two meshes present comparable results, with the 16pix giving more details and the 32

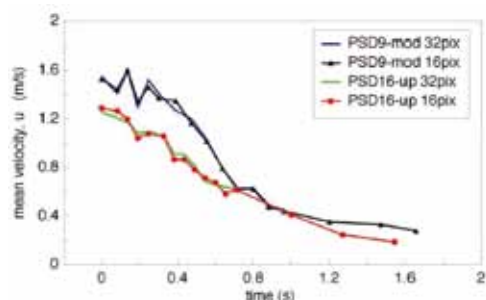


Fig. 10 - Mean velocity versus time

pix providing smoother and more precise results

All the profiles show a non-zero slip velocity at the bottom, of about 0.5 m/s, probably due to the relatively low degree of roughness provided by the material which covers the bed of the flume (with respect to the size of the grains). In all cases, the flows appear to show large shearing toward the base, while they tend to move with a more constant velocity toward the surface. This tendency is more pronounced for PSD16-up-b, which moves with a plug in the upper part of the flow.

DISCUSSION AND CONCLUDING REMARKS

This paper presents the preliminary results of a novel method for measuring the kinematic behaviour of a transparent highly concentrated particle-fluid system moving down an inclined channel, in a ‘free surface’ condition and with relatively high-speed movements. The use of a non intrusive optical approach which relies on the matching of the refractive index of the constituents and planar laser-induced fluorescence (PLIF) techniques, makes the investigation of the field velocity in the inner part of the flow possible.

Digital images recorded during a first series of experiments were obtained with the laser plane positioned 35 mm from the outside face that is $\frac{1}{4}$ of the total width of the employed flume apparatus. It is expected that edge effects during shearing would be significantly reduced at this distance but they would not be entirely eliminated. However, in a narrow channel typical of debris flows, some shearing will always be generated by the side-walls of the channel and it is not the intention of this work to completely eliminate all “edge effects”,

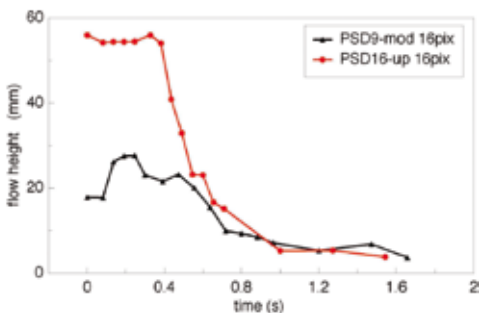


Fig. 11 - Position of the highest patch of each mesh versus time

but only to render visible shearing within the flow. The study of 2-D vertical sections through the interior of the flow allows us to investigate the 3-D dimensional features of the flow inside the bulk.

During an experiment, with a segregating system of particles, the coarser material concentrates at the front of the flow, resulting initially in an unsaturated condition. For this part of the flow it was not possible to use PLIF since the fluid phase is partially absent, however in the body and tail of the flow where the mixture was completely saturated and the solid concentration lower, the observation of the motion of individual particles within the fluid-particle system was possible. A special PIV (Particle Image Velocimetry) technique, GeoPIV, adapted for geotechnical testing and modified to the needs of the present research, has been used to measure the velocity profiles as obtained from laser-illuminated images through the transparent flowing mixture.

Two mixtures with the same sediment volume concentration and mean particle size D_{50} , but consisting different material i.e., a well-graded material with $C_U=20.2$ and a uniform one with $C_U=3.3$, were investigated. The results show that the particle size distribution strongly affects the overall flow behaviour with well-graded material exhibiting greater speed and far greater runout in comparison to uniformly graded mixtures. Also the heights of the flow and velocity profiles measured at the control section of the flume slope were quite different. The well-graded mixture moved downslope the channel as an elongated and thin flow, while the uniform mixture moved as a bulky surge displaying a lower degree of shearing. Further investigations are planned to analyze in detail the influence of the larger particles in the flow behaviour of the well-graded mixtures and to examine the internal shearing behaviour of the flows.

ACKNOWLEDGEMENTS

This research was financially supported through the Royal Society of New Zealand Marsden Fund. The authors would like to thank laboratory staff Messers Siale Faitotonu, John Kooloos, Rob MacGregor, Peter McGuigan, Ian Sheppard and Kevin Wines of the University of Canterbury for help in construction of the flume apparatus and experimental testing. The authors would also like to thank Dr W.A. Take for providing a modified version of GeoPIV for use in the research.

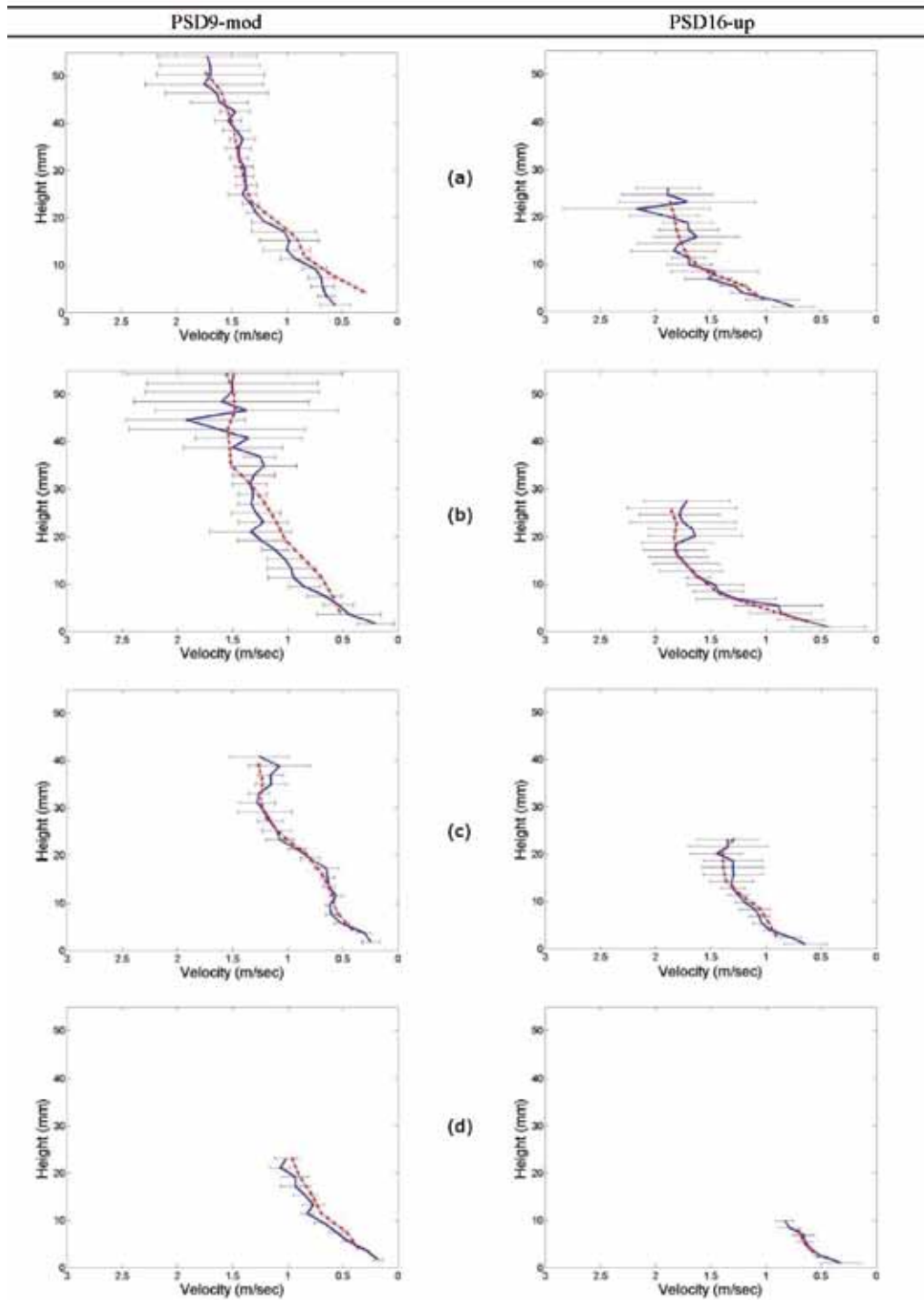


Fig. 12 - Typical velocity profiles for PSD9-mod and PSD16-up at different times for 16pix meshes (solid line) with the corresponding error bars (estimated as standard deviation). The 32pix velocity (dashed line) is overlapped for comparison. (a) and (b) velocity profiles in the body; (c) and (d) velocity profiles in the tail

REFERENCES

- ARMANINI A., DALRI' C., FRACCAROLLO L., LARCHER M. & ZORZIN E. (2003) - *Experimental analysis of the general features of uniform mud-flow*. Proc. 3rd International Conference on Debris-Flow hazard mitigation: mechanics, prediction, and assessment, Davos, 10-12 September 2003, Vol. 1: 423-434, edited by Millpress, Rotterdam 2003.
- ARMANINI A., CAPART H., FRACCAROLLO L. & LARCHER M. (2005) - *Rheological stratification in experimental free-surface flows of granular-liquid mixtures*. Journal of Fluid Mechanics, **532**: 269-319.
- BOWMAN E.T. & SANVITALE N. (2009) - *The Role of Particle Size in the Flow Behaviour of Saturated Granular Materials*. Proc. 17th International Conference on Soil Mechanics & Geotechnical Engineering (ICSMGE), 5-9 October, Alexandria, Egypt. Edited by M.Hamza, S. Marawan and Y. El-Mossallamy. IOS Press, Amsterdam, the Netherlands, 1: 470-473.
- BUDWIG R. (1994) - *Refractive index matching for liquid flow investigations*. Experiments in Fluids, **17**: 350-355.
- FONTENOT M.M. & VIGIL R.D. (2002) - *Pore-scale study of nonaqueous dissolution in porous media using Laser-Induced Fluorescence*. Journal of Colloid and Interface Science, **247**: 481-489.
- HURLIMANN M., RICHENMANN D. & GRAF C. (2003) - *Field and monitoring data of debris flow events in the Swiss Alps*. Canadian Geotechnical Journal, **40**: 161-175.
- IVERSON R.M. (1997) - *The physics of debris flows*. Reviews of Geophysics, **35** (3): 245-296.
- MAINALI A. & RAJARATNAM N. (1994) - *Experimental study of debris flow*. Journal of Hydraulic Engineering, **120**(1): 104-123.
- MAJOR J.J. & IVERSON R.M. (1999) - *Debris-flow deposition - effects of pore-fluid pressure and friction concentrated at flow margins*. Geological Society of America Bulletin, **111**: 1424-1434.
- MONTEMAGNO C.D. & GRAY W.G. (1995) - *Photoluminescent volumetric imaging: A technique for the exploration of multiphase flow and transport in porous media*. Geophysical Research Letters, **22** (4): 425-428.
- ORPE V.O. & KUDROLLI A. (2007) - *Velocity Correlations in Dense Granular Flows Observed with Internal Imaging*. Physical Review Letters, **98** (23): 238001
- PIERSON T.C. (1980) - *Erosion and deposition by debris flows at Mt. Thomas, North Canterbury, New Zealand*. Earth Surface Processes, **5**: 227-247.
- SANVITALE N., BOWMAN E.T. & GENEVOIS R. (2010) - *Optical investigation through a flowing saturated granular material*. Zurich, Switzerland: 7th International Conference on Physical Modelling in Geotechnics (ICPMG 2010), 28 Jun-1 Jul 2010.
- STOHR M., ROTH K. & JAHNE B. (2003) - *Measurement of 3D pore-scale flow in index-matched porous media*. Experiments in Fluids, **35**: 159-166.
- WHITE D.J., TAKE W.A. & BOLTON M.D. (2003) - *Soil deformation measurement using particle image velocimetry (PIV) and photogrammetry*. Geotechnique, **53** (7): 619-631.